

LASER INTERFEROMETER GRAVITATIONAL WAVE OBSERVATORY
- LIGO -
CALIFORNIA INSTITUTE OF TECHNOLOGY
MASSACHUSETTS INSTITUTE OF TECHNOLOGY

Technical Note

LIGO-T0900144-v4-D

Date: 2010/06/07

Advanced LIGO Arm Length Stabilisation System Design

Matt Evans, Peter Fritschel, David McClelland, John Miller, Adam
Mullavey, Daniel Shaddock, Bram Slagmolen, Sam Waldman, et al.

Distribution of this document:

Interferometer Sensing and Control

Draft

California Institute of Technology
LIGO Project, MS 18-34
Pasadena, CA 91125
Phone (626) 395-2129
Fax (626) 304-9834
E-mail: info@ligo.caltech.edu

Massachusetts Institute of Technology
LIGO Project, Room NW17-161
Cambridge, MA 02139
Phone (617) 253-4824
Fax (617) 253-7014
E-mail: info@ligo.mit.edu

LIGO Hanford Observatory
Route 10, Mile Marker 2
Richland, WA 99352
Phone (509) 372-8106
Fax (509) 372-8137
E-mail: info@ligo.caltech.edu

LIGO Livingston Observatory
19100 LIGO Lane
Livingston, LA 70754
Phone (225) 686-3100
Fax (225) 686-7189
E-mail: info@ligo.caltech.edu

<http://www.ligo.caltech.edu/>

Contents

1	Introduction	3
1.1	Supporting Documentation	3
2	Overview	3
2.1	Requirements	3
2.2	Approach	4
2.3	System Components	5
2.3.1	Mirror Coating Modifications	5
2.3.2	In Vacuum TransMon Table	6
2.3.3	Auxiliary Laser Table	6
2.3.4	Vertex Heterodyne Measurements	6
3	ALS System	7
3.1	End Station Phase Stabilisation	7
3.1.1	Fibre Delivery of Phase Reference	8
3.2	Arm locking at 532 nm	8
3.2.1	Frequency Range	8
3.2.2	Mode Matching	10
3.2.3	Beam Steering	10
3.2.4	Beam Interception	10
3.3	Vertex heterodyne measurements	11
3.3.1	Vertex Heterodyne Beat Note Stability	12
3.4	Lock Acquisition Procedure	14
3.4.1	Prerequisites	14
3.4.2	Handover	15
3.5	RF Modulation and RF Electronics	15
4	Single Arm Test at LHO	15
4.1	Hardware List	17
4.2	Electronics	17

A	Version History	21
B	CDS Channels	22
C	Schematic diagram of the ALS Locking Strategy	24
	References	27

1 Introduction

This document describes the design of the Advanced LIGO Arm Length Stabilisation (ALS) system. The related Single Arm Test, to be performed at LHO, is also outlined.

The quadruple suspension system (quad) designed to isolate the test masses, provides attenuation of ground motion at frequencies above 10 Hz. Displacements at frequencies below or near the quadruple suspension's resonant frequencies will not be well attenuated. Even with the BSC ISI platforms, test mass displacements of $\sim 10^{-7}$ m/ $\sqrt{\text{Hz}}$ are expected below 0.5 Hz. Excursions of this size will prevent the actuators mounted on the quad from acquiring lock of the arm cavities in a controllable and repeatable manner. To make lock acquisition more deterministic, the arm cavities are to be locked independently from the central recycling cavities using auxiliary lasers.

This independent arm locking scheme will provide a means of holding the arm cavities off resonance for the main PSL beam, facilitating lock acquisition of the central recycling cavities. Once the recycling cavities are robustly locked, the ALS system will bring the arm cavities onto resonance with the PSL and handover [feedback](#) to the global interferometer sensing and control system.

1.1 Supporting Documentation

- Adv. LIGO Arm Length Stabilisation Requirements ([T0900095-v2](#))
- The advanced LIGO ETM transmission monitor ([T0900385-v6](#))
- Preliminary ALS installation schedule (single arm test) ([E1000101-v1](#))
- Table-Top Frequency Stabilization Servo (TTFSS), [aLIGO Wiki page](#).
- Low Noise Voltage-Controlled Oscillator, [aLIGO Wiki page](#).
- Arm Length Stabilisation, [aLIGO Wiki page](#).
- Core Optics Coating Design Details, [aLIGO Wiki COC Detailed Design](#)

2 Overview

2.1 Requirements

The ALS system requirements are described fully in T0900095. In this section we provide a concise summary.

In order for the independent locking approach to be effective it must reduce the residual rms arm cavity length fluctuations to within one cavity linewidth (FWHM at 1064 nm). In terms of displacement this linewidth is approximately 1.3 nm.

The permissible noise of the auxiliary laser with respect to the PSL is limited by the strength of the quadruple suspension's actuators. This noise level has been conservatively estimated

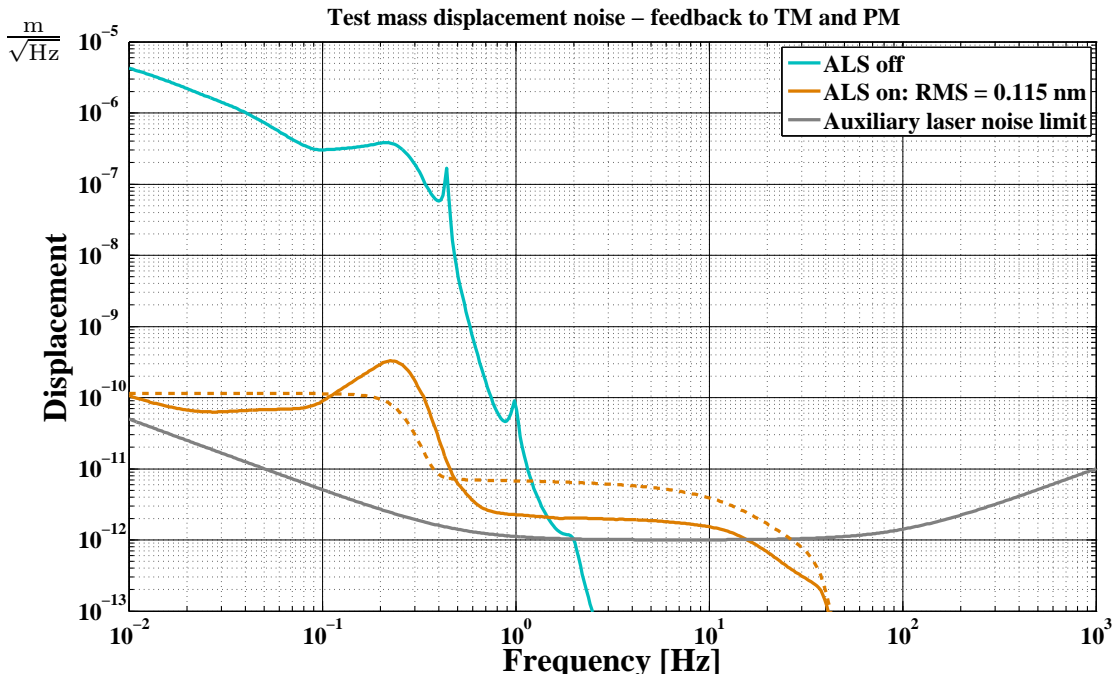


Figure 1: Test mass displacements with the ALS system off (cyan) and on (orange). The permissible noise of the auxiliary laser with respect to the PSL is shown in grey.

by assuming that control forces are restricted to the penultimate mass and test mass (see section 3.4 for more details). The allowable noise floor under these constraints, found via Simulink modelling, is shown in figure 1. The same quantity is given in various units in table 1.

Table 1: ALS auxiliary laser noise limit.

Auxiliary laser noise relative to PSL	$\sim 1 \text{ pm}/\sqrt{\text{Hz}}$ (see figure 1) $\sim 70 \text{ mHz}/\sqrt{\text{Hz}}$ $\sim 70/f \text{ mrad}/\sqrt{\text{Hz}}$
---------------------------------------	--

2.2 Approach

The auxiliary laser at the end station outputs beams at two wavelengths – 1064 nm and 532 nm. The 1064 nm beam is used to ensure that the auxiliary laser is phase locked to the PSL, and the 532 nm beam is used to lock the auxiliary laser to the arm cavity.

Once locked, the 532 nm beam transmitted by the arm cavity is employed in a heterodyne measurement with a frequency doubled sample of the PSL beam used to provide feedback to control the common and differential length of the arm cavities.

In this state, introducing a tunable offset into the 532 nm heterodyne locking loop allows

Table 2: Optical transmission in the vertex at 532 nm.

Optic or path	T 532 nm	Comment
ETM HR	5.1%	Provided by LMA
ETM AR	-	Provided by LMA
ITM HR	1.0%	Provided by LMA
ITM AR	76%	Provided by LMA
X Path, s-pol	30%	Path: After ITM AR surface to reflection from PR3 (CSIRO)
Y Path, s-pol	15%	Path: After ITM AR surface to reflection from PR3 (CSIRO)
X _{folded} Path, s-pol	10%	Path: After ITM AR surface to reflection from PR3 (CSIRO)
Y _{folded} Path, s-pol	21%	Path: After ITM AR surface to reflection from PR3 (CSIRO)
PR2 HR	59%	Provided by ATF
PR2 AR	99.78%	Provided by ATF
Arm Cavity Finesse	~100	

2.3.2 In Vacuum TransMon Table

The TransMon Table houses the ETM Transmission Monitor Telescope. The table is approximately 23" \times 40" (600 mm \times 1000 mm) in size and is suspended from the BSC ISI platform immediately behind the ETM's quad suspension.

The ETM telescope is a 16:1 ratio beam reducing telescope, supporting both the 1064 nm and 532 nm beams. QPDs for the transmitted 1064 nm beam are situated on this table. There is also a Hartmann beam pick off which captures the 532 nm reflection from the wedged AR surface of the ETM and directs it through one of the viewports. For greater detail regarding the design and layout of the TransMon table see [1, 2, 3].

2.3.3 Auxiliary Laser Table

The Auxiliary Laser Table is a 4 ft \times 8 ft optical table located adjacent to the vacuum chamber in the end station. The auxiliary dual-wavelength laser (1064/532 nm) and associated injection optics are located on this table. In addition the heterodyne measurement between the auxiliary laser and PSL beam, transferred to the end station via optical fibre, will be performed on this table. The auxiliary laser table will be XX cm away from the chamber with its surface at a height of 30" (760 mm). Further details regarding the optical layout of the auxiliary table are presented in section 3.2.

2.3.4 Vertex Heterodyne Measurements

Once each arm cavity is locked to its auxiliary laser, the 532 nm beams transmitted by the arm cavities are extracted at PR2 and routed to the PSL table. Two heterodyne measurements are performed. One between the X arm transmission and a doubled sample of the PSL and one between the X arm and Y arm transmissions. The output of these two measurements is used to provide 'common mode' and 'differential mode' error signals re-

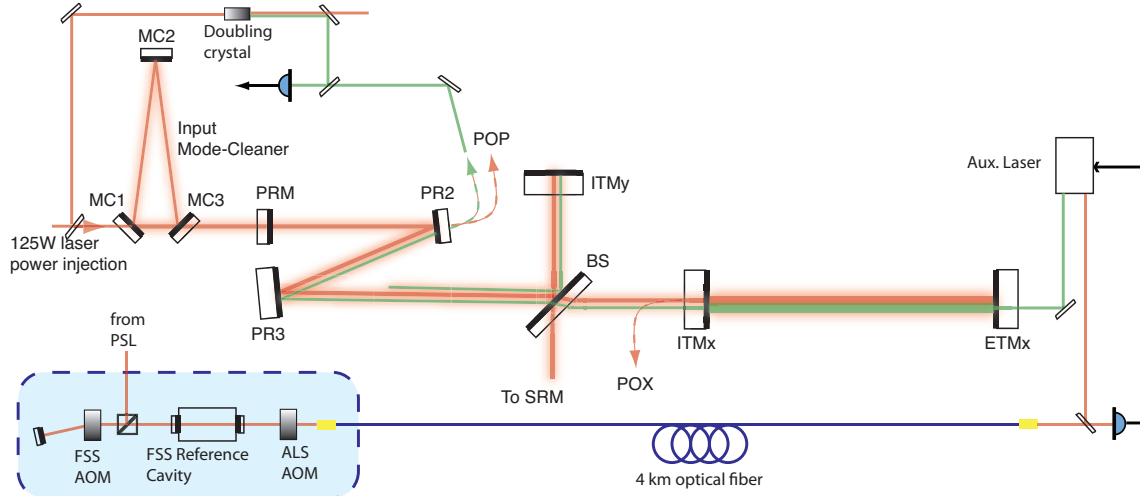


Figure 3: Transfer of the PSL phase reference to the auxiliary laser at the end stations.

spectively. The ‘common mode’ signal is directed to the input mode cleaner common mode board servo. The ‘differential mode’ signal is used to feedback to the ETMs. The result is that the auxiliary laser is locked to the PSL with low noise across all frequencies of interest (see section 3.3).

3 ALS System

3.1 End Station Phase Stabilisation

To allow for a smooth transition of arm cavity control from ALS to global interferometer signals, the auxiliary laser must have a well defined phase relationship with the PSL. A robust phase locked loop is an integral part of this scheme. The physical implementation of the first stage of this loop is explained below.

A portion of the beam transmitted by the reference cavity is used as a PSL phase reference and relayed to the end stations via existing optical fibres. This beam is frequency shifted by 79.4 MHz by a double pass AOM upstream of the reference cavity (part of the FSS). After the reference cavity, the beam is down shifted in frequency by 158.8 MHz prior to injection into the fibre, see figure 3.

In the end-station the fibre output is then combined with the 1064 nm output of the auxiliary laser to generate a heterodyne beat note at 39.475 MHz. This beat note is used to phase lock the auxiliary laser to the PSL. The phase locked loop servo is based around a TTFSS servo. Control signals are sent to the laser PZT and temperature controller, limiting bandwidth to approximately 50 kHz.¹ The heterodyne beat note is demodulated using a Low Noise VCO.

Figure 4 illustrates the layout of the auxiliary laser table. The 1064 nm output is prepared

¹If wider bandwidth is found to be desirable, a Pockels cell can be introduced to the 1064 nm beam path. This would not affect the 532 nm light directly unless an external SHG were to be used in place of the Prometheus laser.

in the standard way by wave plates and a Faraday isolator. The nominal output power of ~ 1 W is reduced to a more manageable level by a partially transmissive mirror before a half wave plate and polarising beam splitter (PBS) provide finer adjustment. Approximately 1 mW will be used for heterodyne measurements with the fibre output. Excess power is directed onto a high power beam dump.

3.1.1 Fibre Delivery of Phase Reference

The existing fibre running from the LVEA to the end stations is known to be single mode for 1310/1550 nm and may also be single mode for 1064 nm. If multimode operation is observed new fibre which is single mode at 1064 nm will be purchased.

Transmission through 4 km of fibre will introduce an equivalent frequency noise of approximately $100 \text{ Hz}/\sqrt{\text{Hz}}$ (flat up to 100 Hz) [4]. We do not implement an explicit fibre noise cancellation system as the feedback from the vertex heterodyne measurements to the ETMs (see section 3.3) will indirectly suppress the fibre induced phase noise.

The purpose of the PSL-auxiliary laser PLL is simply to maintain the frequency of the auxiliary laser close to that of the PSL at low frequency so that, once the arm cavities are locked, the beat notes measured on the PSL table fall within the photodetectors' bandwidths.

3.2 Arm locking at 532 nm

Once the auxiliary laser is locked to the fibre transmission, the 532 nm output of the auxiliary laser is locked to the arm cavity using PDH reflection locking. Control signals act on the ~ 40 MHz VCO supplying the phase locked loop's local oscillator, tuning the offset of auxiliary laser with respect to the fibre output. This loop will utilise standard common mode servo electronics and is expected to have a bandwidth of a few kHz.

The polarisation of the 532 nm beam is linearised by two wave plates before it passes through a Faraday isolator. Phase modulation sidebands are then added to enable PDH readout. Table 3 lists the modulation frequencies utilised for all six interferometer arms.

The beam is subsequently injected through a mode matching (and Gouy phase) telescope, via the TransMon table, into the arm cavity. The reflected beam is extracted using a second Faraday isolator.

We estimate that the 532 nm beam will undergo a total attenuation of 50% (due to 2x Faraday isolators, $T \sim 80\%$; 1x Hartmann pick off, $T \sim 90\%$; 1x TransMon pick off, $T \sim 95\%$; 3x TransMon dichroics, $T \sim 97\%$) before reaching the ETM. In order to realise our desired input power of ~ 10 mW, we require a power output of approximately 20 mW at 532 nm from the auxiliary laser.

3.2.1 Frequency Range

Initially the 532 nm laser output is locked to the arm cavity length. In order to follow the arm cavity length fluctuations, the 532 nm laser must have adequate control authority.

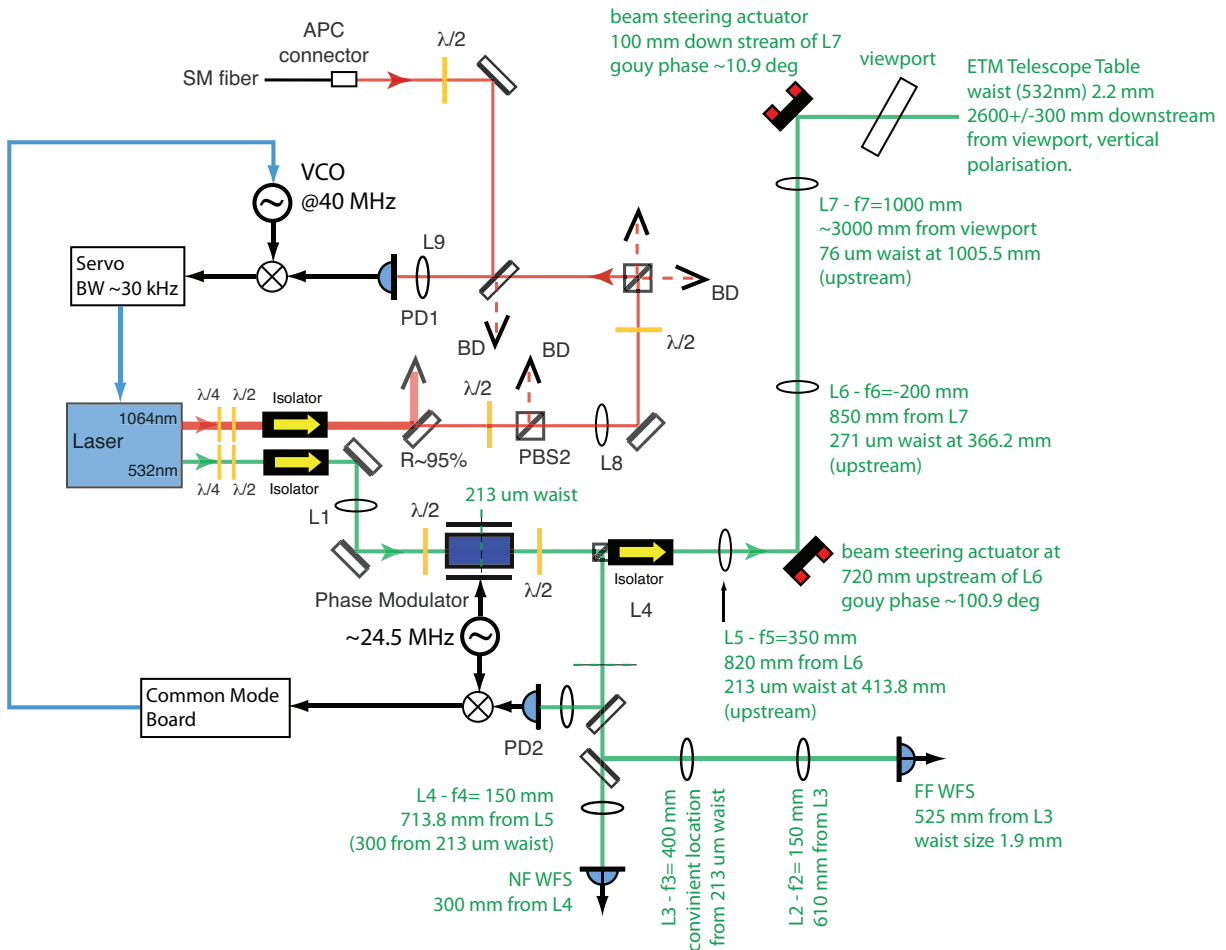


Figure 4: Layout of the end station laser table. The auxiliary laser is stabilised to the fibre output using the 1064 nm beam with feedback sent to the laser actuators (PZT and temperature). The 532 nm laser output is mode matched and locked to the arm cavity, by introducing an offset into the 1064 nm PLL. The high gain LSC detectors sampling the arm cavity transmission are omitted for clarity.

The required actuation is dominated by displacements of the test masses at low frequency. To ensure that the ALS system can acquire lock of the arm cavities even when other subsystems (e.g. BSC ISI) are not functioning we demand that the 532 nm laser output frequency be tunable over ± 705 kHz. This value stems from an effective displacement requirement of ± 5 μm .

$$\Delta\nu = \frac{\delta x c}{\lambda L} = \frac{\pm 5 \times 10^{-6} \cdot 3 \times 10^8}{532 \times 10^{-9} \cdot 4 \times 10^3} = \pm 705 \text{ kHz} \quad (1)$$

This frequency range can be accommodated by the Low Noise VCO driving the 40 MHz heterodyne demodulation which has a tuning range of ± 1 MHz.

3.2.2 Mode Matching

The 532 nm beam is mode matched into the TransMon telescope (and therefore the arm) by a Galilean style telescope located on the in air optical table. The telescope consists of a converging $f=1000$ mm lens and a diverging $f=200$ mm lens (lenses L7 and L6 in figure 4 respectively). The lens separation is optimised such that a beam undergoes a predetermined Gouy phase advance on propagation through the telescope. One two-axis PZT steering mirror is located on either side of the telescope. The Gouy phase difference between the two actuation positions is nominally 90° .

The waist of the TransMon telescope for 532 nm is 2.2 mm, located 2.6 ± 0.3 m from the viewport. The propagation distance from the viewport to the first steering mirror on the optical table (including a 300 mm periscope) is ~ 3 m [1]. Our mode matching solution assumes a 213 μm waist inside the phase modulator (see figure 4).

3.2.3 Beam Steering

DC QPDs on the TransMon table will guide initial alignment of the 532 nm ALS beam into the arm cavity and monitor ALS injection beam alignment. Differential wavefront sensing will subsequently be employed to align the auxiliary laser beam to the arm cavity. Figure 4 reveals the positions of both the near field (NF) and the far field (FF) wavefront sensors (WFSs) and their associated Gouy phase telescopes. These telescopes are designed to provide 90° Gouy phase difference between the detector locations, permitting orthogonal sensing of beam tilts and offsets. Alignment control signals derived from these quadrant diodes will be applied to the PZT steering mirrors on either side of the mode matching telescope.²

3.2.4 Beam Interception

Three beams leave the vacuum envelope to arrive on the optical table at the end station (see figure 10). The main 1064 nm science beam transmitted through the arm cavity (during lock acquisition and initial alignment this beam will be directed onto a high gain QPD), the auxiliary 532 nm beam used for the arm length stabilisation and a second 532 nm beam, the reflection from the wedged AR surface of the ETM, part of the Hartmann sensor system. The high gain photodiode and Hartmann sensor optics will not be discussed in this document.

²Nano-MTA2 actuators from Mad City Labs are currently being investigated.

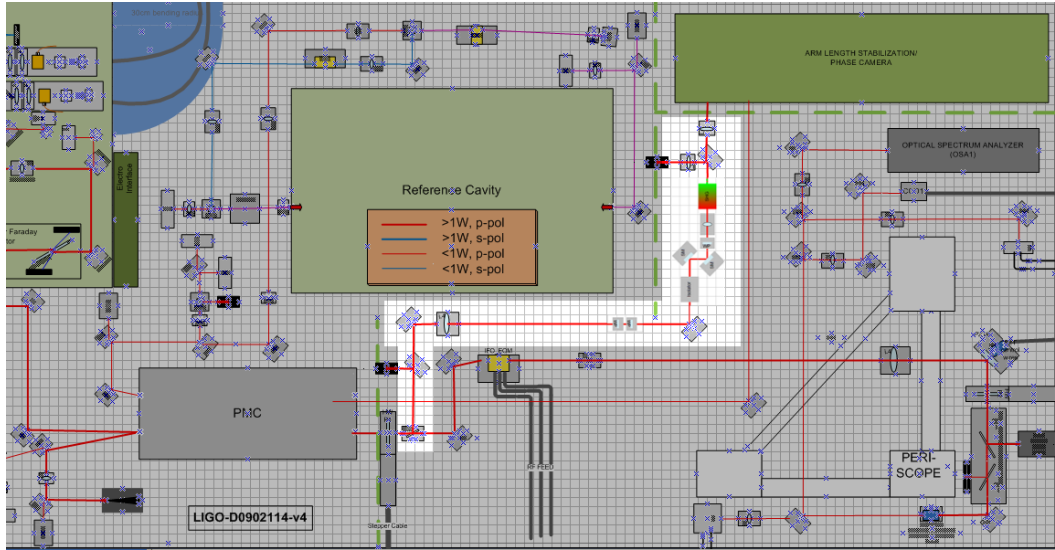


Figure 5: Schematic of the PSL table showing the ALS pick off (just after the PMC, bottom left). The ALS system will extract 1 Watt of power and pass it through a SHG to produce ~ 4 mW at 532 nm (LIGO-D0902114-v4).

All three beams exit the BSC chamber at a downward angle of 20° from horizontal. Each beam will be intercepted by a separate 300 mm tall periscope supporting 2" optics. Upon exiting the periscope all beams will have a nominal height of 4" and propagate parallel to the optical table. The heights of the periscopes' primary mirrors can be adjusted to accommodate any variations in the heights of the beams exiting the chamber.

3.3 Vertex heterodyne measurements

Once locked on resonance, the 532 nm beams transmitted by the arm cavities propagate via the beamsplitter, reflection from PR3 and transmission through PR2 (see figure 3) to the PSL table.

On resonance, the cavity power transmission will be $\sim 50\%$ (see table 1). Using table 2, the attenuation on propagation from cavity output to transmission through PR2 will be $\sim 91\%$ (for the Y Path in s-polarisation).³ This yields an available power on the PSL table of ~ 44 μ W.

Figure 5 illustrates how the ALS system will interface with the PSL and IO subsystems on the PSL table. Approximately 1 W of power is diverted to ALS by a partially transmissive mirror downstream of the PMC. This beam is passed through a SHG to provide ~ 4 mW of 532 nm light.⁴

This doubled beam is employed in a heterodyne measurement comparing its phase to that of the 532 nm light transmitted by the X arm. The local oscillator for this measurement has a frequency of 78.95 MHz.

³Compared to 34ppm away from resonance.

⁴The IR beam transmitted through the SHG crystal is made available for the phase cameras.

Draft

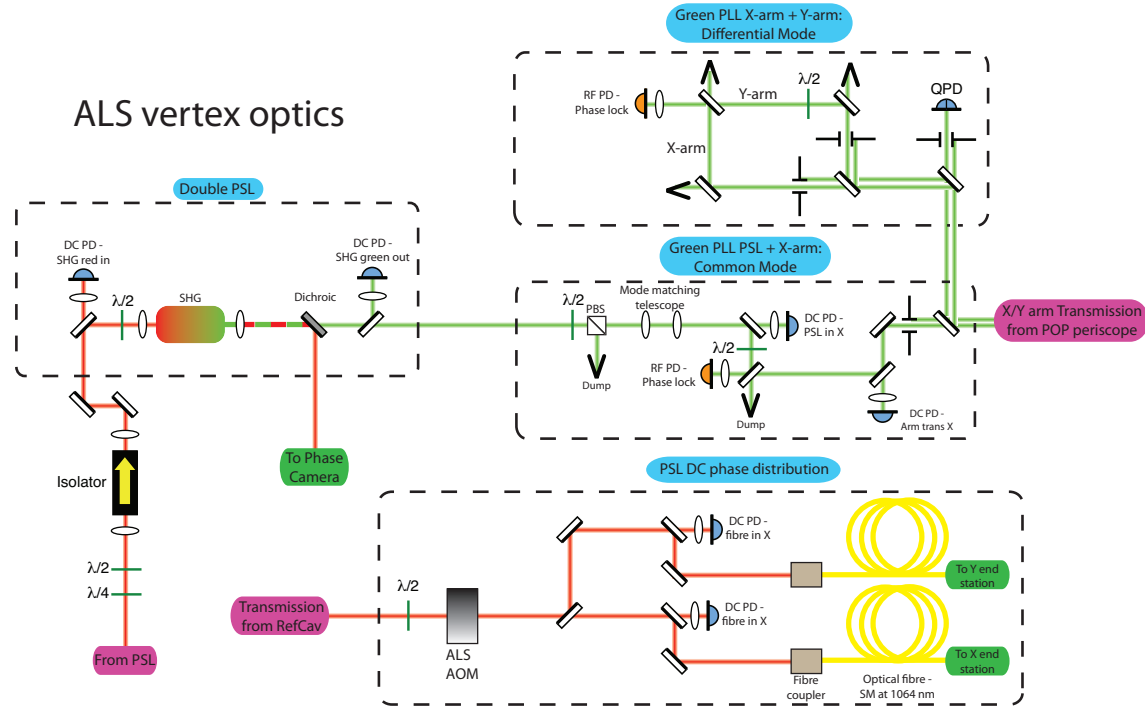


Figure 6: Layout of the heterodyne beat note measurement in the vertex, as well as the PSL fibre injection.

The error signal from this loop is filtered and routed to second input on the common mode board servo, providing feedback to the input mode cleaner and the VCO controlling the 79.4 MHz AOM of the PSL Frequency Stability Servo (FSS). This feedback path is termed the ‘common mode’ path in the ALS scheme.

A second heterodyne measurement is obtained by combining the beams transmitted by both arm cavities. On the PSL table these beams are only $\sim XX$ mm apart, they will be separated by appropriately placed apertures.

Demodulation at 157.9 MHz uncovers the phase difference between the two transmitted beams. This signal is digitised and sent to the end stations via the reflective memory network where it is fed back to the ETMs differentially. This control path is referred to as the ‘Differential Mode’ in the ALS scheme.

A schematic of the ALS vertex optics is presented in figure 6.

3.3.1 Vertex Heterodyne Beat Note Stability

Figure 7 shows the maximum tolerable phase noise for the vertex local oscillators. This limit is obtained by converting the ‘Auxiliary laser noise limit’ displacement in figure 1 to phase

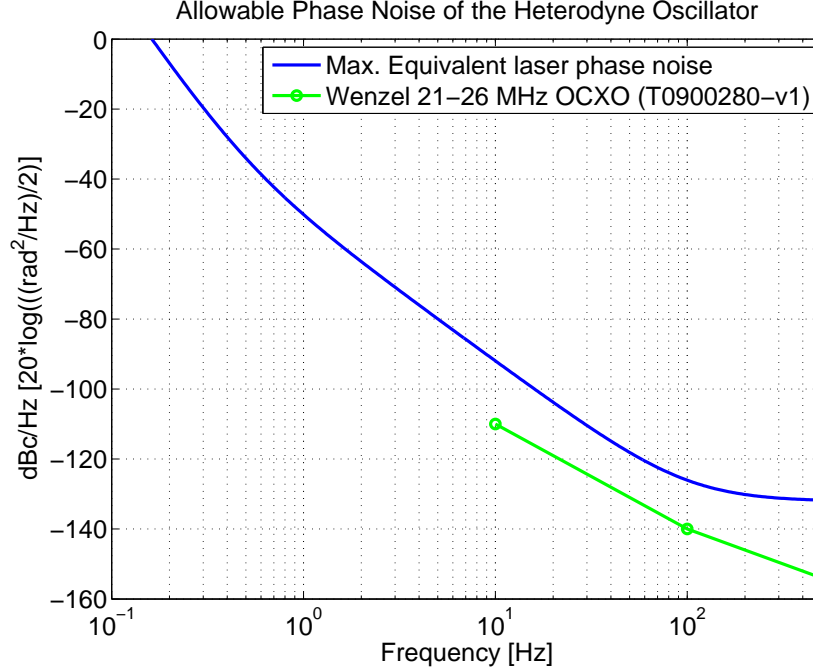


Figure 7: Permissible RF local oscillator phase noise (solid blue) and phase noise of the Wenzel 500-14927 OCXO oscillator used in the RF Oscillator Source (green with circles, see figure 9).

noise relative to carrier through (page 768, [5])

$$S(f) = 20 \log \left(\frac{\phi^2(f)}{2} \right) \quad [\text{dBc/Hz}], \quad (2)$$

$$\text{where } \phi(f) = \frac{\delta x(f) \nu}{L_{\text{arm}} f} \quad [\text{rad}/\sqrt{\text{Hz}}]. \quad (3)$$

Here $\delta x(f)$ is the displacement limit from figure 1, ν is the laser frequency (at 532 nm) in Hz, L_{arm} is the arm cavity length in m and f is the Fourier frequency in Hz.

Figure 7 also shows the phase noise of the Wenzel 500-14927 (21-26 MHz-AT Streamline Crystal Oscillator) OCXO stable oscillator used to drive our RF oscillator source. The OCXO noise is a factor of ~ 3 below the modelled noise limit. An additional 10x noise reduction is achieved by using two VCO modules in series (with a compromise of a reduction in dynamic range to 100 kHz).

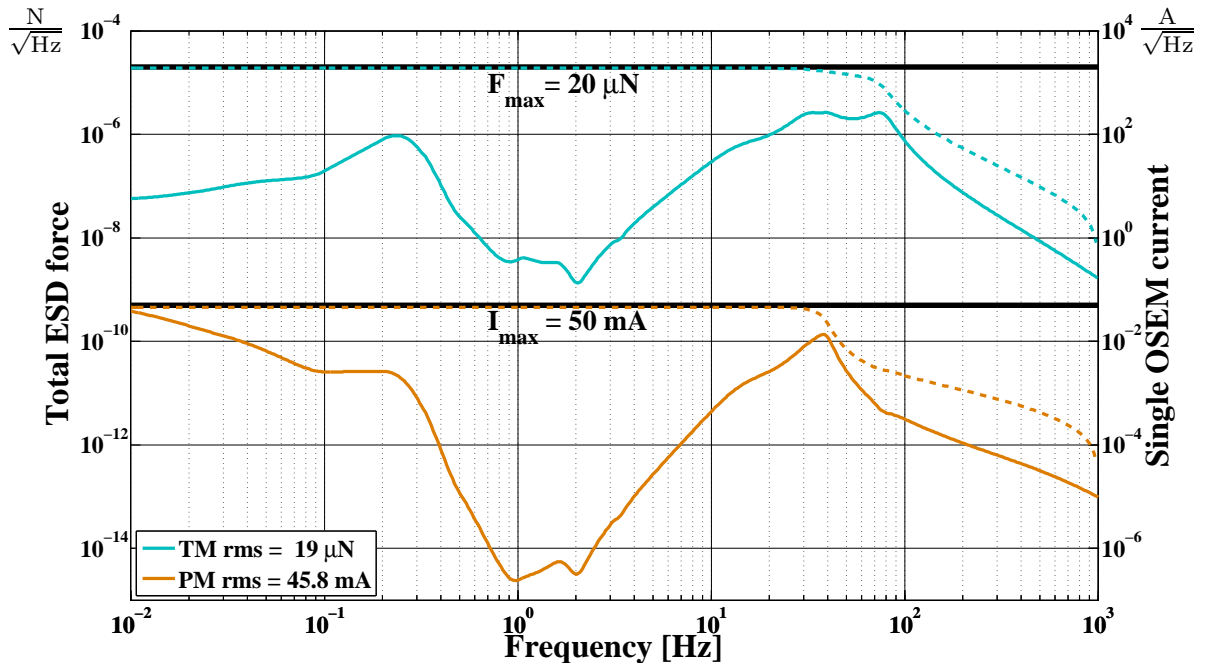


Figure 8: Residual arm motion can be suppressed below the ALS requirement (1.3 nm rms) without saturating the quad suspension actuators. In this investigation control signals were routed to the penultimate mass and test mass only. The solid traces represent the amplitude spectral density of the actuation signals (A/\sqrt{Hz} or N/\sqrt{Hz}) while the dashed lines represent the integrated rms values (Ampere or Newton). Horizontal black lines indicate reasonable limits placed on rms coil current and ESD force.

3.4 Lock Acquisition Procedure

3.4.1 Prerequisites

Four loops must be closed before the transition to global interferometer control signals can begin:⁵

1. PSL-Auxiliary laser 1064 nm PLL
2. Arm cavity lock at 532 nm
3. Vertex ‘common mode’
4. Vertex ‘differential mode’

In addition the residual arm length fluctuations must not exceed 1.3 nm rms. Simulink modelling has shown that this criterion can be met with a realistically noisy auxiliary laser, feeding back to only the penultimate and test masses (see figures 1 and 8).

⁵We neglect auxiliary loops e.g. SHG phase matching, arm cavity alignment etc.

Once arm length fluctuations have been reduced to within one cavity linewidth (at 1064 nm) it is possible to maintain the global (i.e. not ALS) cavity error signals within their linear ranges and a controlled handover can commence.

3.4.2 Handover

The demodulations involved in the ALS ‘common’ and ‘differential’ modes (see section 3.3) are controlled by VCOs. Each of these oscillators accepts DC inputs which can be tuned to offset the common and differential modes of the interferometer arm cavities.

Initially offsets are introduced to facilitate acquisition of the short degrees of freedom by preventing the PSL beam from resonating in the arm cavities. Once these cavities are under global control, the arm cavity offsets will be reduced in a controlled manner and ALS common and differential mode control will be passed to standard interferometer CARM and DARM signals.

3.5 RF Modulation and RF Electronics

The RF modulation frequencies chosen for the ALS system were selected to allow initial LIGO ISC photodetectors and wavefront sensors to be used. As a result all modulation frequencies lie around 24.5 MHz (see table 3).

Table 3: ALS RF modulation frequencies.

IFO	X arm	Y arm
H1	24.407079 MHz	24.482125 MHz
L1	24.407079 MHz	24.482125 MHz
H2	24.440707 MHz	24.515730 MHz

A block diagram of the ALS electronics system is presented in figure 9. A complete list of necessary components is given in table 4.

4 Single Arm Test at LHO

The Hanford Single Arm Test involves the installation and commissioning of a single Advanced LIGO arm cavity. Building upon work carried out at LASTI, this investigation will explore the integrated control of the quadruple suspensions, BSC ISIs and HEPIs. The ALS system plays a central role in this test, its auxiliary laser providing a means of measuring cavity displacement noise.

The frequency noise of the auxiliary laser is expected to be the dominant noise source in the Single Arm Test. To mitigate this effect the laser will be stabilised to a monolithic reference cavity using a Table Top Frequency Stabilisation Servo (TTFSS). This will not have the

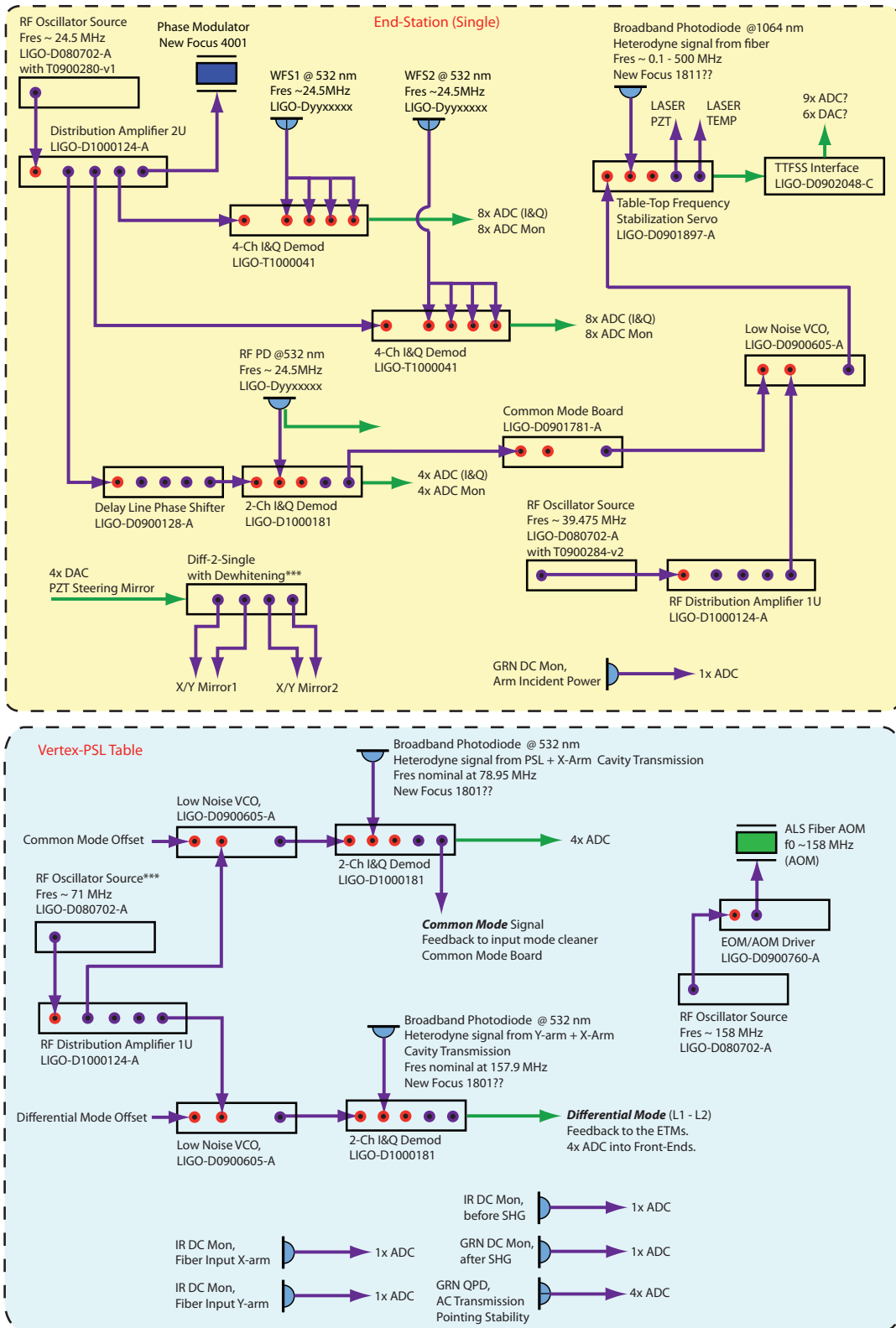


Figure 9: Diagram of ALS electronics. Top: Single end station; Bottom: Vertex layout for both arms.

Table 4: ALS RF components (see figure 9).

Chassis	DCC Number	Qty/IFO
RF Oscillator Source	D080702-A	6
Distribution Amplifier 1U	D1000124-A	3
TTFSS	D0901897-A	2
TTFSS Interface	D0902048-C	2
4-Ch I&Q Demodulator	T1000041	4
2-Ch I&Q Demodulator	T1000181	4
Delay Line Phase Shifter	D0900128-A	2
Common Mode Board	D0901781-A	2
Low Noise VCO	D0900605-A	4
EOM/AOM Driver	D0900760-A	3
LSC Photodetector (532 nm)	Dyyxxxxx	2
LSC Photodetector Interface	D0901833-B	2(?)
WFS (532 nm)	Dyyxxxxx	4
WFS Interface	Dyyxxxxx	4
Broadband Detectors (1064 nm)	xxxxxx	2
Broadband Detectors (532 nm)	xxxxxx	2

same performance as the ALS requirement, but will provide means to investigate the BSC ISI and Quad control up to frequencies up to ~ 0.5 Hz.⁶

To lock the auxiliary laser to the arm cavity, a double passed AOM is placed in the path to the reference cavity. Acting on the AOM's VCO allows the laser frequency to be adjusted indirectly through the reference cavity control loop.

Figure 10 shows the optomechanical layout (to scale) of the in air table.

The anticipated schedule for ALS installation prior to the Single Arm Test is available in [6].

4.1 Hardware List

Table 5 list the hardware required for ALS system/Single Arm Test.

4.2 Electronics

Figure 11 presents a block diagram of the Single Arm Test electronic components. Two principal control loops exist, the first being the laser frequency stabilisation servo (shown in the middle 'blue' box. A Table Top Frequency Stabilisation Servo is used to lock the laser to a standard initial LIGO style reference cavity. Control signals are applied to the laser temperature and PZT.

The second main loop locks the laser to the arm cavity by tuning the RF drive frequency

⁶This has been modelled and shown on the aLIGO 'Arm Length Stabilisation' wiki page.

Table 5: ALS and Single Arm Test (SAT) hardware (Baseline - 1 IFO)

Item	Part	Vendor	Location	Qty	Spare	Total Qty	SAT Qty
Prometheus Laser 1W @1064 nm & 100mW @532nm		InnoLight GmbH	End	2	1	3	1
Faraday Isolator at 1064nm	IO-3-1064-HP	OFR/Thorlabs	Vertex/End	3	0	3	1
PBS@1064nm	PBS-1064-050	CVI	End	3	0	3	1
Beam splitter @1064nm (50/50 P-pol)	BS1-1064-50-1012-45-S	CVI	End	2	2	4	3
Steering Mirrors @1064nm - 1"	Y1-1025-45-UNP	CVI	End	10	1	11	2
Steering Mirrors @1064nm - 2"	Y1-2037-45-UNP	CVI	Vertex/end	24	4	28	9
Lenses @1064nm	PLCX-25.4-178.5-C-1064 (for example)	CVI	Vertex/end	2	2	4	1
Half wave plate @1064nm (zero order)	QWPO-1064-05-2-R10	CVI	Vertex/end	20	2	22	8
Quarter wave plate @1064nm (zero order)	QWPO-1064-05-4-R10	CVI	Vertex/end	8	2	10	5
Beam Dumps @1064	AOM-402AF4	LIGO	Vertex/end	4	2	6	2
AOM - 40 MHz @1064nm	AOM-	IntraAction Corp.	End	10	5	15	5
AOM - 80 MHz @1064nm	AOM-4002	IntraAction Corp.	End	0	0	0	1
Phase Modulator - 21.5 MHz @1064nm		New Focus	End	0	0	0	1
Reference Cavity + Vacuum enclosure		LIGO	End	0	0	0	1
Optical Table 4 ft x 8 ft + enclosure + legs		Newport	End	1	0	1	1
Faraday Isolator at 532nm (5mm aperture)	I-56T-5M	ISOWAVE	End	4	0	4	2
PBS @532nm	PBS-532-050	CVI	End	6	1	7	2
Beamsplitters @532nm (50/50)	BS1-532-50-1025-45-S	CVI	End/Vertex	6	2	8	3
Steering Mirrors @532nm - 1"	Y2-1025-45-S	CVI	End	30	4	34	6
Steering Mirrors @532nm - 2"	Y2-2037-45-S	CVI	End	10	0	10	5
Lenses @532nm (1" and 2")	PLCX-25.4-178.5-C-532 (for example)	CVI	End	31	4	35	10
Half wave plate @532nm (zero order)	QWPO-532-05-2-R10	CVI	End	14	2	16	5
Quarter wave plate @532nm (zero order)	QWPO-532-05-4-R10	CVI	End	2	2	4	1
Phase Modulator @532nm (24 MHz)	4001	New Focus	End	2	0	2	1
Fast Steering Mirror + Driver	Nano-MTA2	Mad City Labs	End	4	0	4	2
Non-linear crystal (single pass)	LiNb/PPKTP?		Vertex	1	2	3	
Crystal Holder with oven/Peltier element			Vertex	1	0	1	
Temp Controller			Vertex	1	0	1	
Dichroic HR@1064 nm	AR@532 nm		Vertex	1	2	3	
Mount for Faraday Isolators	Block for ISOWAVE FI	ANU	End	7	0	7	3
Mount for PM	9071	New Focus	End	2	0	2	1
Mount for AOM	SN100-F3K	New Focus	End/Vertex	0	0	0	2
BS/Mirror Mounts - 1"	SS100-F2K	Newport	Vertex/End	16	3	19	5
Mirror Mounts - 1"	SL51BM	Newport	Vertex/End	54	8	62	15
Mirror Mounts - 2"	RSP1 + TR2	Thorlabs	End	8	2	10	5
Wave plate mount + 2" post	LMR1 + TR2	Thorlabs	Vertex/end	28	8	36	13
Lens Mounts - 1" + 2" post		Thorlabs	Vertex/End	51	6	57	18
PBS Mounts		Newport	Vertex/End	8	3	11	5
Post/base for 1" mirror mount (4" beam height)	D0901749-v1-C& 0.75" diameter post	LIGO/ANU	Vertex/End	70	11	81	20
Post/base for 2" mirror mount	D0901749-v1 -C& 0.75" diameter post	LIGO/ANU	Vertex/End	10	0	10	5
Base PBS mount (variable height)	Q-TMS-2	Newport	End	8	3	11	5
Post PBS mount & 1" diameter, 2" length	PS-2E	Newport	End	8	3	11	5
Post/base for Wave plate Lens + Mounts (4")	PH2	Thorlabs	Vertex/End	79	14	93	31
Base - mounting plate	BA2	Thorlabs	Vertex/End	159	25	184	56
Clamp L-shape	CL5	Thorlabs	Vertex/End	318	50	368	112
Grub Screw	#8-32 x xx"	Thorlabs	Vertex/End	80	11	91	25
SHCS 1/4-20 x 0.5"			Vertex/End	80	20	100	10
SHCS 1/4-20 x 3/8"			Vertex/End	79	20	99	10

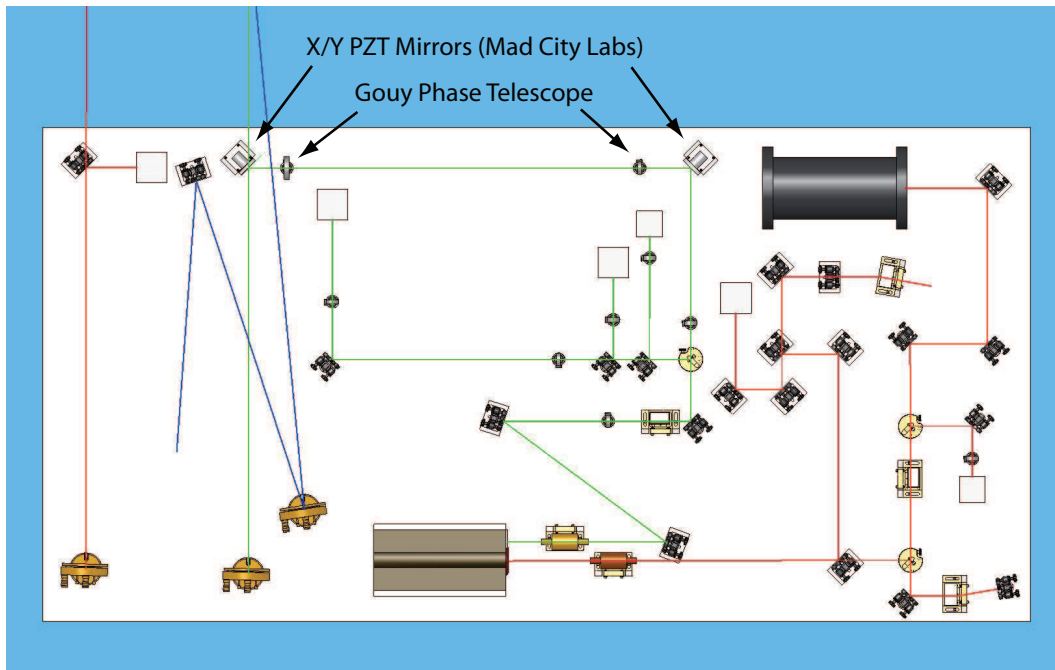


Figure 10: Schematic of the In Air optical table.

sent to the AOM. This provides a means of locking the laser frequency to the arm cavity, whilst simultaneously maintaining lock of the reference cavity to suppress the laser frequency noise.

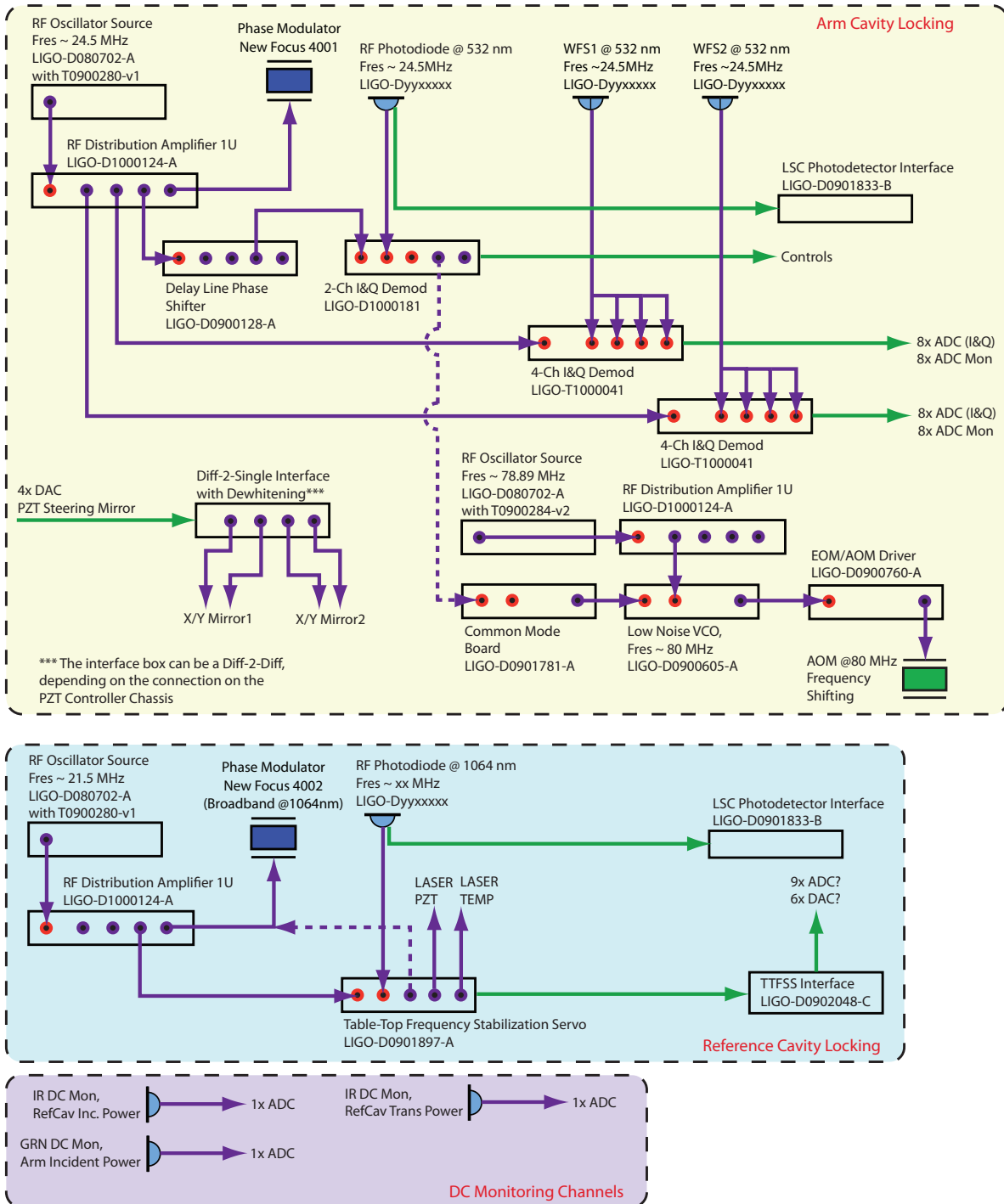


Figure 11: Block diagram of Single Arm Test electronics. Top: RF electronics for locking the laser to the arm cavity. Middle: Layout for locking the laser to the reference cavity. Bottom: DC photodiodes.

Table 6: Single Arm Test RF components (see figure 11).

Chassis	DCC Number	Qty	Reused in ALS
RF Oscillator Source (with T0900280-v1)	D080702-A	2	yes (need 18)
RF Oscillator Source (with T0900284-v1)	D080702-A	1	no
Distribution Amplifier 1U	D1000124-A	3	yes (need 6)
TTFSS	D0901897-A	1	yes (need 6)
TTFSS Interface	D0902048-C	1	yes (need 6)
4-Ch I&Q Demodulator	T1000041	2	yes (need 12)
2-Ch I&Q Demodulator	T1000181	1	yes (need 12)
Delay Line Phase Shifter	D0900128-A	1	no
Common Mode Board	D0901781-A	1	no
Low Noise VCO (~ 80 MHz)	D0900605-A	1	no
EOM/AOM Driver	D0900760-A	1	no
LSC Photodetector (532 nm)	Dyyxxxxx	2	yes (need 6)
LSC Photodetector (1064 nm)	xxxxx	2	no
LSC Photodetector Interface	D0901833-B	4(?)	(need 6)
WFS (532 nm)	Dyyxxxxx	4	yes (need 12)
WFS Interface	Dyyxxxxx	4	yes (need 12)

A Version History

-v1

Initial release

-v2

- Started appendix A ‘Version History’.
- Modified section 3.2.1 to reflect what is mentioned in the ALS Requirements Document (T0900095-v2).
- Updated figures with the latest fibre phase noise suppression measurements.
- Updated figure 4, include the mode matching telescope for the 532 nm beam and wavefront sensors.

-v3

- Modified the introduction to include a discussion of the vertex green heterodyne beat note scheme.
- Made small changes to the Approach section.
- Removed section 6 In-Vacuum-TransMon-Table.

- Modified section 2.3.2 ‘In-Vacuum TransMon-Table’.
- Updated ‘System Overview’.
- Removed fibre phase noise cancellation implementation and results.
- Added the Single Arm Test.
- Included the RF building blocks.

-v4

- Removed the approach section to reduce repetition.
- Inserted transmission table 2.
- Section 3.2.1, change the dynamic range from $1 \mu\text{m}_{pk}$ to $\pm 5 \mu\text{m}$ (e.g. 10 μm peak to peak).
- Included stable Quad feedback using the penultimate mass and the test mass only.
- Major reshuffle of the sections.
- Made the Quad VCO locking strategy the baseline locking approach.

B CDS Channels

Required CDS channels from ALS_CDS_ADC_DAC.xls.

ALS_CDS_ADC_DAC_Channels.xls

ADC/DAC Channels for the Arm Length Stabilisation System (incl. the fiber noise cancellation scheme)

Total ADC Cards (Corner and 2x End Stations) 3

Total DAC Cards (Corner and 2x End Stations) 3

ADC Channels - End Station

Item	Ch. Per item	Item Qty	Total
Tip-Tilt Actuator	4	2	8
Sensors Act. Mon.	2	2	
WFS	8	2	16
DC power error signal	4	4	
PD (green)	1	2	2
DC power error signal	1	1	
PDH Error (green)	1	1	1
DC power error signal	1	1	
PD (IR)	1	2	2
DC power error signal	1	1	
PDH Error (IR)	1	1	1
DC power error signal	1	1	
Fiber Noise PD	1	2	2
DC power error signal	1	1	

Total ADC Channels 32
Total ADC Cards (32 ch) 1

ADC Channels - Corner Station

Item	Ch. Per item	Item Qty	Total
Fiber Noise PD	1	4	4
DC power error signal	1	1	
Fiber Noise Error	1	2	2
error signal	1	1	

Total ADC Channels 6
Total ADC Cards (32 ch) 1

Bram Slagmolen

Page 1/1

7/7/09

DAC Channels - End Station

Item	Ch. Per item	Item Qty	Total
Tip-Tilt Actuator	2	2	4
Actuators	2	2	
Laser	3	2	6
PZT	1	1	
Temp	1	1	
Temp Offset	1	1	

Total DAC Channels 10
Total DAC Cards (15 ch) 1

DAC Channels - Corner Station

Item	Ch. Per item	Item Qty	Total
Fiber Noise PD	1	2	2
VCO	1	1	
Fiber Noise Pol. Contro	1	2	2
Pol. Rotator	1	1	

Total DAC Channels 4
Total DAC Cards (15 ch) 1

Figure 12: Required CDS channels including fibre noise cancellation scheme.

C Schematic diagram of the ALS Locking Strategy

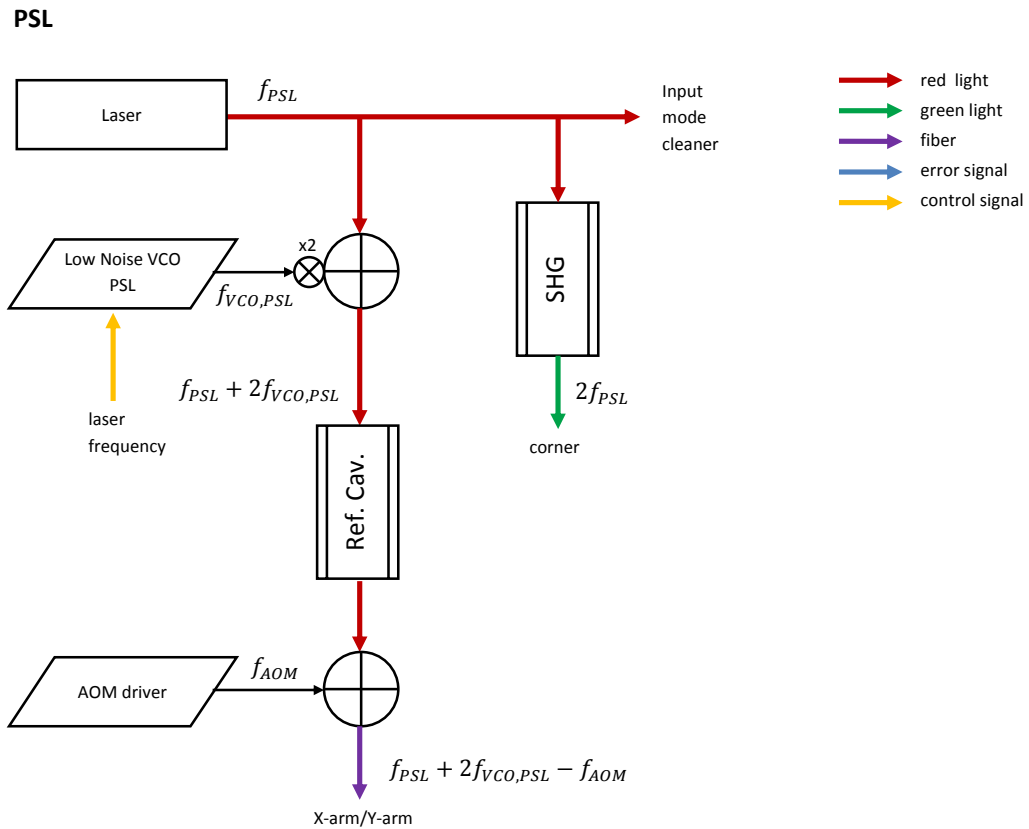


Figure 13: Schematic of Opto-Electronic for the ALS locking strategy on the PSL table.

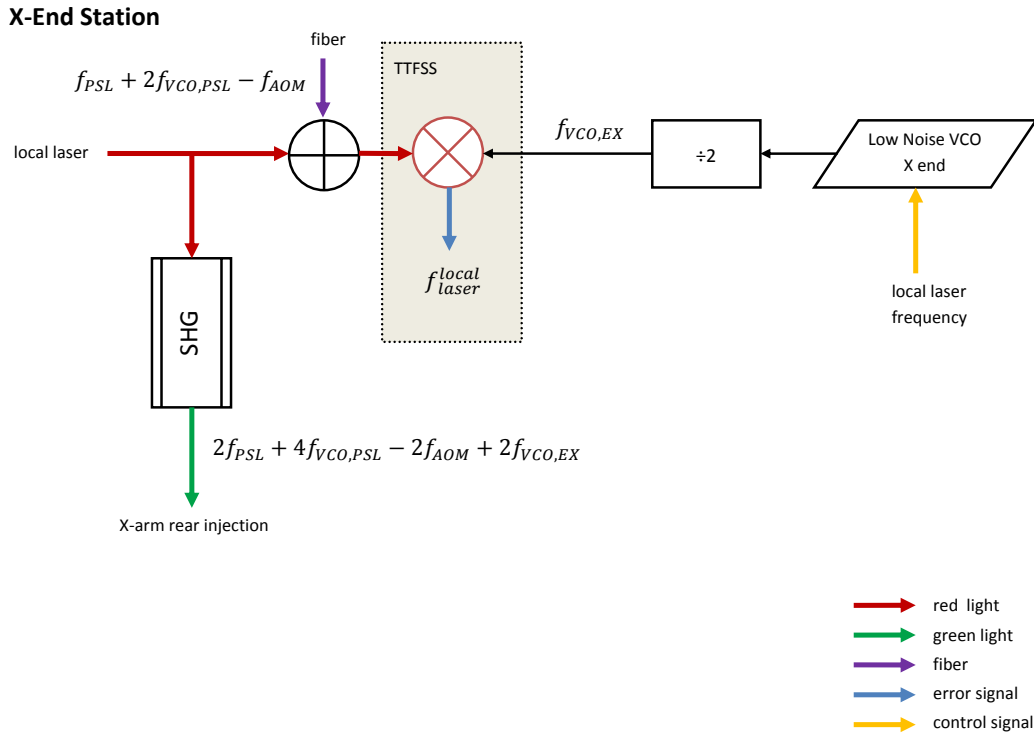


Figure 14: Schematic of Opto-Electronic for the ALS locking strategy in the End-Station.

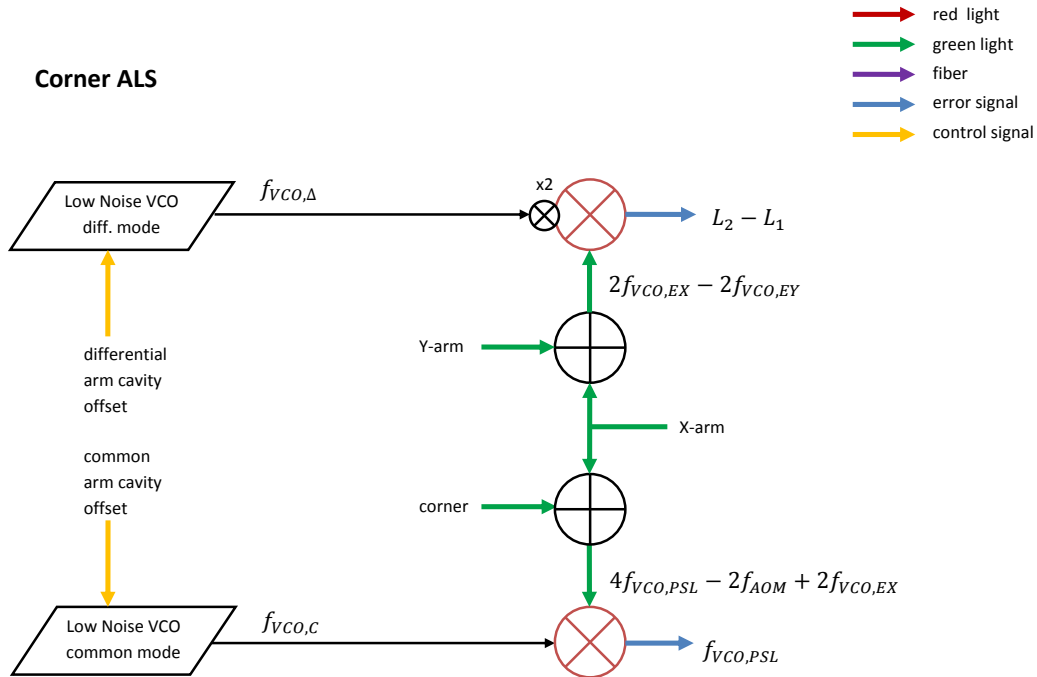


Figure 15: Schematic of Opto-Electronic for the ALS locking strategy on the PSL table.

Table 7: Demodulation frequencies for the ALS Locking Strategy

Frequency	Equation	Nominal (MHz)
Laser towards mode cleaner (1064 nm)	f_{PSL}	0.000
Low noise VCO at PSL	$f_{VCO,PSL}$	79.400
In transmission of reference cavity	$f_{REF} = f_{PSL} + 2f_{VCO,PSL}$	158.800
AOM at fiber launch	f_{AOM}	158.800
Fiber at end stations	$f_{PSL} + 2f_{VCO,PSL} - f_{AOM}$	0.000
Low noise VCO at X end station	$f_{VCO,EX}$	39.475
Light of X end station laser (1064 nm)	$f_{PSL} + 2f_{VCO,PSL} - f_{AOM} + f_{VCO,EX}$	39.475
Light of X end station laser (532 nm)	$2f_{PSL} + 4f_{VCO,PSL} - 2f_{AOM} + 2f_{VCO,EX}$	78.950
Low noise VCO at Y end station	$f_{VCO,EY}$	-39.475
Light of Y end station laser (1064 nm)	$f_{PSL} + 2f_{VCO,PSL} - f_{AOM} - f_{VCO,EY}$	-39.475
Light of Y end station laser (532 nm)	$2f_{PSL} + 4f_{VCO,PSL} - 2f_{AOM} - 2f_{VCO,EY}$	-78.950
Light after SHG in corner (532 nm)	$2f_{PSL}$	0.000
Interference X arm/corner	$4f_{VCO,PSL} - 2f_{AOM} + 2f_{VCO,EX}$	78.950
Interference Y arm/corner	$4f_{VCO,PSL} - 2f_{AOM} - 2f_{VCO,EX}$	-78.950
Interference X arm/Y arm	$2f_{VCO,EX} - 2f_{VCO,EY}$	157.900
Common mode low noise VCO	$f_{VCO,C} = 2f_{VCO,EX} + \Delta f_C$	
Differential mode low noise VCO	$f_{VCO,D} = 2f_{VCO,EX} + 2f_{VCO,EY} + 2\Delta f_D$	
Demodulated common mode	$4f_{VCO,PSL} - f_{AOM} - \Delta f_C$	
Demodulated differential mode	$-2\Delta f_D$	

References

- [1] S. J. Waldman. The Advanced LIGO ETM transmission monitor. *LIGO-T0900385-v6*, 2010.
- [2] P. Fritschel and S. Waldman. Requirements and Interfaces for the ETM Transmission Monitor Suspension and Telescope. *LIGO-T0900265-v1*, 2009.
- [3] S. Waldman and M. Smith. Advanced LIGO Transmon Zemax. *LIGO-D0900446-v11*, 2009.
- [4] Dick Gustafson, Ewan Douglas, Peter Fritschel, and Sam Waldman. Fiber Phase Noise Measurements at LHO. *LIGO-T0900376-v1*, August 2009.
- [5] Paul Young. *Electronic Communication Techniques*. Ignatius Press, San Francisco, 1999.
- [6] John Miller. Preliminary ALS installation schedule (single arm test). *LIGO-E1000101*, March 2010.